Chapter 11
Statistical Analysis for Liutex Growth in Flow Transition

Charles Nottage, Yifei Yu, and Chaoqun Liu

Abstract In computational fluid dynamics, many researchers and textbooks accepted that vorticity is vortex. However, this is a misunderstanding of the tensors derived from the Cauchy-Stokes decomposition of the velocity gradient tensor. It was believed that the symmetric tensor A and antisymmetric tensor B (vorticity tensor) represented stretching/compression and rotation, respectively. Decomposing the vorticity tensor yields R (rotation part) and S (antisymmetric shear deformation part). Liutex, on the other hand, represents rigid rotation and the Liutex magnitude represents twice the angular speed. We analyze three flow areas in boundary-layer transition: laminar, transitional, and turbulent. In laminar flow, there is no vortex structure. In transitional flow, the formation of hairpin vortex rings will begin. Finally, in turbulent flow, many vortex rings have formed. In this paper, a DNS simulation of boundary transition is conducted, then statistical analysis is performed on the recorded results for Liutex, shear, and vorticity. The resulting values for Liutex followed the proper growth trend, starting at zero in laminar flow and steadily increasing through the transitional and turbulent flows. On the other hand, the vorticity values were much greater and remained consistent with little change throughout the flow transition periods. The analysis also revealed that the shear component negatively relates with Liutex, i.e., as Liutex increases, shear decreases. Since shear substantially impacts the vorticity value where it can be misrepresented as rotation in laminar flow, vorticity, in general, should not be considered vortex.

11.1 Introduction

A vortex is recognized as the rotational motion of fluids. Many vortex identification methods have been developed within the last several decades to track the vortical structure in a fluid flow; however, we still lacked unambiguous and universally accepted vortex identification criteria. This obstacle caused a lot of confusion and misunderstandings in turbulence research [1]. These methods are characterized

C. Nottage (✉) · Y. Yu · C. Liu
Department of Mathematics, The University of Texas at Arlington, Arlington, TX 76019, USA
e-mail: charles.nottage@mavs.uta.edu

into three generations starting with vorticity-based methods as the first generation, eigenvalue-based such as Δ [2, 3], Q [4], λ_2 [5], λ_{ci} [6], and Ω [7, 8], as the second generation, and the recently developed Liutex methods as the third generation of vortex identification methods [9]. The Liutex method is a novel eigenvector-based method that is local, accurate, unique, and systematic [10].

In Computational fluid dynamics, many researchers and textbooks accept that vorticity is vortex. This is due to a misunderstanding from the Cauchy-Stokes decomposition of the velocity gradient tensor. It was understood that the symmetric tensor A represented stretching/compression, and the antisymmetric tensor B (vorticity tensor) represented rotation [11]. In this paper, we will show that antisymmetric tensor B (vorticity tensor) does not represent only rotation and investigate the behavior of shear, Liutex, and vorticity in the boundary layer from laminar flow to turbulent flow.

This manuscript is split into sections, where Sect. 11.2 is a review of vorticity and Liutex, Sect. 11.3 shows that vorticity is not strictly rotation, Sect. 11.4 shows the data structure for the DNS study, and Sect. 11.5 is the results of the investigation of the behavior of shear Liutex, and vorticity.

11.2   Review of Related Vortex Identification Methods

The vortex identification methods that we will analyze in this paper are vorticity and Liutex. We will review these methods in this section.

11.2.1   Vorticity

In 1858, Helmholtz introduced the concept of the vorticity tube/filament [12]. Since then, many researchers have believed that vortices consist of small vorticity tubes called vortex filaments, and the magnitude of vorticity gives the vortex strength.

11.2.1.1   Vorticity Vector

The vorticity vector is mathematically defined as the curl of the velocity. i.e.,

$$\text{vortivity} = \nabla \times \vec{\mathbf{v}} = \begin{vmatrix} \mathbf{i} & \mathbf{j} & \mathbf{k} \\ \frac{\partial}{\partial x} & \frac{\partial}{\partial y} & \frac{\partial}{\partial z} \\ u & v & w \end{vmatrix}$$

$$= \mathbf{i}\left(\frac{\partial w}{\partial y} - \frac{\partial v}{\partial z}\right) - \mathbf{j}\left(\frac{\partial w}{\partial x} - \frac{\partial u}{\partial z}\right) + \mathbf{k}\left(\frac{\partial v}{\partial x} - \frac{\partial u}{\partial y}\right) \qquad (11.1)$$

The vorticity vector is also derived as follows [5]:

$$\vec{\omega} = \nabla \times \vec{v} = \left(\frac{\partial}{\partial x}, \frac{\partial}{\partial y}, \frac{\partial}{\partial z}\right)^T \times (u, v, w)^T$$

$$= \left(\frac{\partial w}{\partial y} - \frac{\partial v}{\partial z}, \frac{\partial u}{\partial z} - \frac{\partial w}{\partial x}, \frac{\partial v}{\partial x} - \frac{\partial u}{\partial y}\right)^T. \tag{11.2}$$

11.2.1.2 Vorticity Magnitude

The vorticity magnitude is defined as

$$\|\vec{\omega}\| = \sqrt{\left(\frac{\partial w}{\partial y} - \frac{\partial v}{\partial z}\right)^2 + \left(\frac{\partial u}{\partial z} - \frac{\partial w}{\partial x}\right)^2 + \left(\frac{\partial v}{\partial x} - \frac{\partial u}{\partial y}\right)^2}. \tag{11.3}$$

11.2.1.3 Vorticity Tensor

The vorticity tensor is the antisymmetric tensor $\boldsymbol{B}$ from the traditional Cauchy-Stokes decomposition of the velocity gradient tensor $\nabla \vec{v}$ [13]:

$$\boldsymbol{B} = \frac{1}{2}\left(\nabla\vec{v} - \nabla\vec{v}^T\right) = \begin{bmatrix} 0 & \frac{1}{2}\left(\frac{\partial u}{\partial y} - \frac{\partial v}{\partial x}\right) & \frac{1}{2}\left(\frac{\partial u}{\partial z} - \frac{\partial w}{\partial x}\right) \\ \frac{1}{2}\left(\frac{\partial v}{\partial x} - \frac{\partial u}{\partial y}\right) & 0 & \frac{1}{2}\left(\frac{\partial v}{\partial z} - \frac{\partial w}{\partial y}\right) \\ \frac{1}{2}\left(\frac{\partial w}{\partial x} - \frac{\partial u}{\partial z}\right) & \frac{1}{2}\left(\frac{\partial w}{\partial y} - \frac{\partial v}{\partial z}\right) & 0 \end{bmatrix}. \tag{11.4}$$

11.2.2 Liutex

Liutex [9, 10] is a vector defined as $\vec{R} = R\,\vec{r}$. R represents the Liutex magnitude defined as twice the angular velocity, and $\vec{r}$ represents the directional unit vector of Liutex. According to Wang [14], $\vec{r}$ is the real eigenvector of the velocity gradient tensor, and the explicit formula of R is

$$R = \vec{\omega} \cdot \vec{r} - \sqrt{(\vec{\omega} \cdot \vec{r})^2 - 4\lambda_{ci}^2} \tag{11.5}$$

Liutex, as a vector, overcomes the drawbacks of the scalar methods, e.g., the threshold requirement when creating and analyzing graphics.

11.3 Vorticity Versus Rotation

In this section, we will decompose vorticity in the principal coordinate to show that vorticity is not strictly rotational.

11.3.1 Vorticity Tensor in the Principal Coordinate

The Vorticity tensor in the Principal Coordinate has the following form:

$$\boldsymbol{B}_{PC} = \begin{bmatrix} 0 & \frac{1}{2}\left(\frac{\partial U}{\partial Y} - \frac{\partial V}{\partial X}\right) & \frac{1}{2}\left(\frac{\partial U}{\partial Z} - \frac{\partial W}{\partial X}\right) \\ \frac{1}{2}\left(\frac{\partial V}{\partial X} - \frac{\partial U}{\partial Y}\right) & 0 & \frac{1}{2}\left(\frac{\partial V}{\partial Z} - \frac{\partial W}{\partial Y}\right) \\ \frac{1}{2}\left(\frac{\partial W}{\partial X} - \frac{\partial U}{\partial Z}\right) & \frac{1}{2}\left(\frac{\partial W}{\partial Y} - \frac{\partial V}{\partial Z}\right) & 0 \end{bmatrix}$$

$$\boldsymbol{B}_{PC} = \begin{bmatrix} 0 & -\frac{R+\varepsilon}{2} & -\frac{\xi}{2} \\ \frac{R+\varepsilon}{2} & 0 & -\frac{\eta}{2} \\ \frac{\xi}{2} & \frac{\eta}{2} & 0 \end{bmatrix} \tag{11.6}$$

and can be decomposed further into this form:

$$\boldsymbol{B}_{PC} = \begin{bmatrix} 0 & -\frac{R}{2} & 0 \\ \frac{R}{2} & 0 & 0 \\ 0 & 0 & 0 \end{bmatrix} + \begin{bmatrix} 0 & -\frac{\varepsilon}{2} & -\frac{\xi}{2} \\ \frac{\varepsilon}{2} & 0 & -\frac{\eta}{2} \\ \frac{\xi}{2} & \frac{\eta}{2} & 0 \end{bmatrix} = \boldsymbol{R} + \boldsymbol{AS}. \tag{11.7}$$

where $\boldsymbol{R}$ & $\boldsymbol{AS}$ represent the rotation and antisymmetric shear deformation part, respectively. This implies that the vorticity tensor is not strictly rotation [15].

11.3.2 Vorticity Vector in the Principal Coordinate

Using Eq. 11.2 from Sect. 11.2.1.1 and applying the Principal Coordinate yields:

$$\vec{\omega} = \nabla \times \vec{\boldsymbol{v}}_{\theta} = \left(\frac{\partial}{\partial X}, \frac{\partial}{\partial Y}, \frac{\partial}{\partial Z}\right)^{T} \times (U, V, W)^{T}$$

$$= \left(\frac{\partial W}{\partial Y} - \frac{\partial V}{\partial Z}, \frac{\partial U}{\partial Z} - \frac{\partial W}{\partial X}, \frac{\partial V}{\partial X} - \frac{\partial U}{\partial Y}\right)^{T}$$

$$= \left(\eta, -\xi, \frac{R}{2} + \varepsilon - \left(-\frac{R}{2}\right)\right)^T = (\eta, -\xi, R + \varepsilon)^T$$

$$= (\eta, -\xi, \varepsilon)^T + (0, 0, R)^T = \vec{S} + \vec{R} \tag{11.8}$$

where $\vec{R}$ is a rotational vector and $\vec{S}$ is a non-rotational shear vector. This implies that $\vec{\omega}$ contains shearing and rotation components. Therefore, the vorticity vector is not strictly rotational [5, 11, 16].

11.3.3   Vorticity Magnitude in the Principal Coordinate

The vorticity magnitude in the Principal Coordinate is

$$\| \vec{\omega} \| = \sqrt{(\eta)^2 + (\xi)^2 + (R + \varepsilon)^2}. \tag{11.9}$$

The vorticity magnitude contains rotation R and shearing components η, ξ, ε; therefore, the vorticity magnitude does not only represent rotational strength [11].

11.4   Data Structure

The computational domain has the grid number $1920 \times 128 \times 241$, representing the number of grids in streamwise (x), spanwise (y), and wall-normal (z) directions. In normal direction, these grids are stretched, while in streamwise and spanwise directions, they are uniform. The length of the first grid interval in the normal direction at the entrance is 0.43 in wall units (Z+ = 0.43) (see Fig. 11.1).
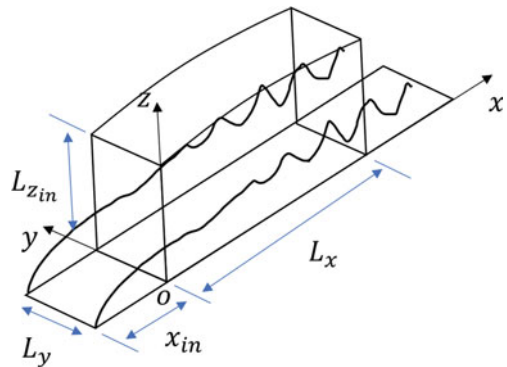
Fig. 11.1 Computation domain

Table 11.1 DNS parameters

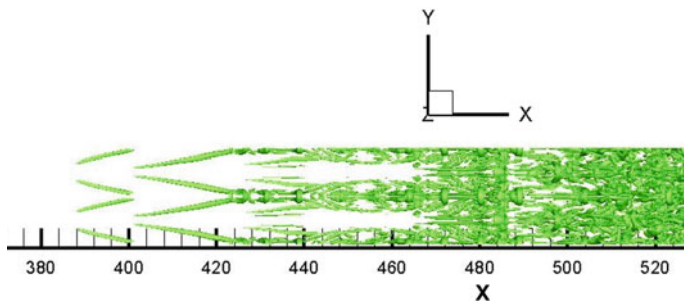| M_∞	Re	x_{in}	Lx	Ly	Lz_{in}	T_w	T_∞
0.5	1000	300.79 δ_{in}	798.03 δ_{in}	22 δ_{in}	40 δ_{in}	273.15 K	273.15 K

Fig. 11.2 Vortex structures by modified Liutex-Omega with $\widetilde{\Omega}_L = 0.52$ at t = 13.00 T

The flow parameters are listed in Table 11.1. Here, M_∞ is Mach number, Re is Reynolds number and, T_w and T_∞ are wall and free stream temperature, respectively. Likewise, x_{in} represents the distance between the leading edge and the inlet of the flat plate. Lx, Ly and Lz_{in} are the lengths of computational domain in x, y, and z directions. δ_{in} is the inflow displacement thickness [1, 17].

Figure 11.2 shows the formation of the vortex structures from the Y direction view in laminar, transitional, and turbulent flow. In laminar flow, little to no vortex activity is detected. In transitional flow, the formation of hairpin vortex rings begins, and this is where weak to strong vortex activity starts to be detected. Then in turbulent flow, many vortex rings have formed. This area is more chaotic and complicated. This means the strength of the vortex should increase from laminar flow to turbulent flow. According to Dong et al., the spanwise Y direction is the most prominent since it contributes the most to the value of the magnitudes [8].

11.5 Results

There are two objectives of this study; by using the DNS simulation of boundary layer transition we:

1. Investigate the behavior of shear, Liutex, and Vorticity from laminar flow to turbulent flow.
2. Analyze the effect of shear on vorticity.

Statistical analysis is performed over the whole grid domain and across time domain T. The Statistical integration formula is

$$\sum_i \sum_j \sum_k \tau_{ijkt} vol_{ijk} = \iota_t, \tag{11.10}$$

where τ_{ijkt} is a point in the grid, $i = 1$ to 1920, $j = 1$ to 128, $k = 1$ to 241 and t represents the step-in time. vol_{ijk} is the volume of the space around the point τ_{ijkt}. ι_t is the integration output value at time step t.

The results of the Direct Numerical Simulation are recorded, Statistical Analysis is performed over the whole grid domain, and the data is plotted across time domain **T** for:

- l_{mag} = Liutex magnitude component
- ω_{mag} = Vorticity magnitude component
- s_{mag} = Shear magnitude component
- l_y = Liutex component in the y direction
- ω_y = Vorticity component in the y direction
- s_y = Shear component in the y direction

The difference in the values of vorticity and Liutex is significantly high, so the relative values are used to compare the change in the values over period **T**.

Figures 11.3 and 11.4 show the behavior of vorticity, shear, and Liutex from the y direction. It is observed that the relative l_y values increased significantly over period **T**, which is the T-S wave period. While ω_y showed no significant change throughout period **T**. The s_y values were observed to be decreasing. This change is negative in nature and coincides with the increase in l_y and the behavior of ω_y. The period **T** travels from laminar flow to turbulent flow. There should be minuscule rotation or vortex activity in laminar flow and an increasing trend of vortex activity as we move into transitional flow, where hairpin vortex rings are formed, and on to turbulent flow. This behavior only coincides with the behavior of the l_y relative values.

It can be observed from Figs. 11.5 and 11.6 that the relative change in l_{mag} across time is much greater than ω_{mag}. As we moved from laminar flow to turbulent flow in time, the values of l_{mag} continually increased, showing that l_{mag} picked up the formation of vortex rings, whereas ω_{mag} barely changed.

11.6 Conclusion

The effect of shear on vorticity can be substantial, leading to a misrepresentation of vortex indication in the laminar flow where there is basically no rotation. The Y direction graphs show that vorticity had little to no change in value over time, while Liutex increased as time progressed. The shear was observed to be decreasing as Liutex increased. This shows that Liutex has a negative relation with Shear deformation. The magnitude graphs show that the increase in Liutex as time progressed is more significant than the increase in vorticity and shear. Therefore, vorticity should not be considered as Vortex.
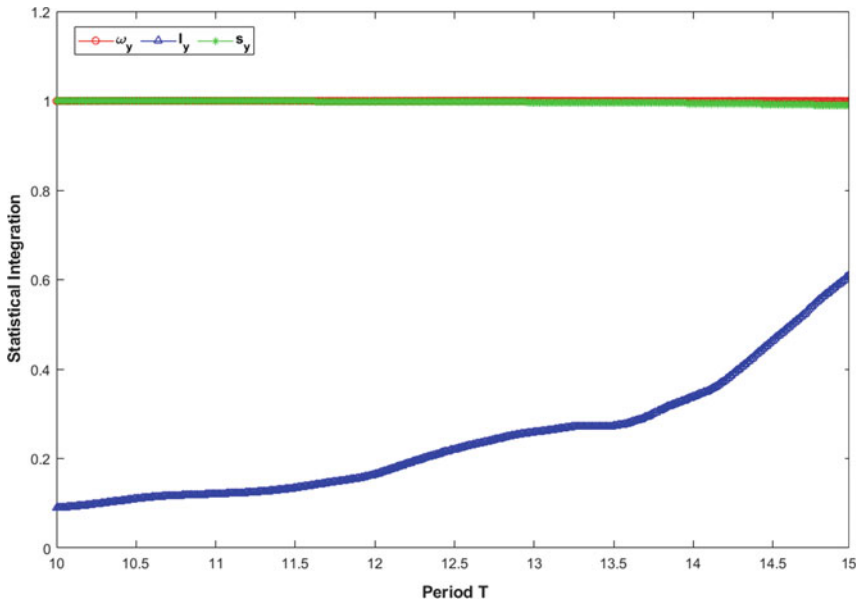
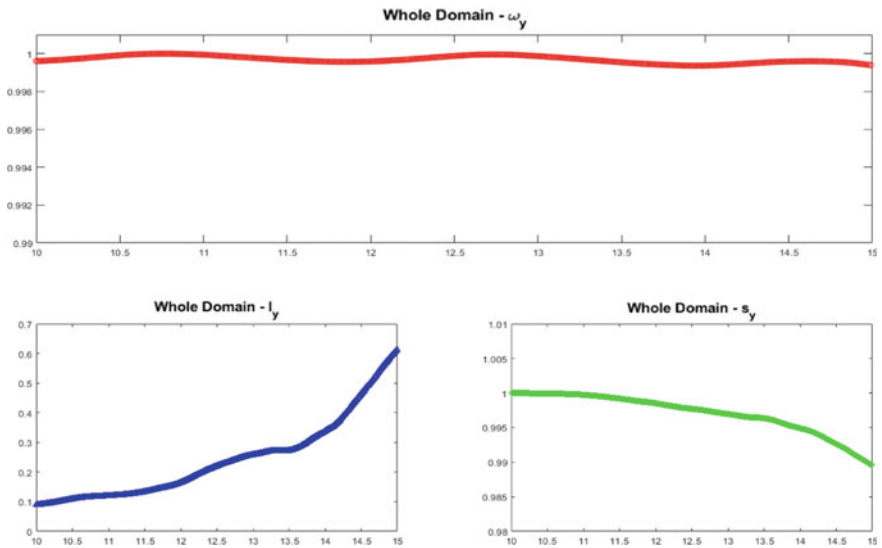**Fig. 11.3** Relative integration values for ω_y, l_y & s_y plotted over time domain **T**

Fig. 11.4 Relative integration values for ω_y, l_y & s_y plotted over time domain **T - individual graphs**
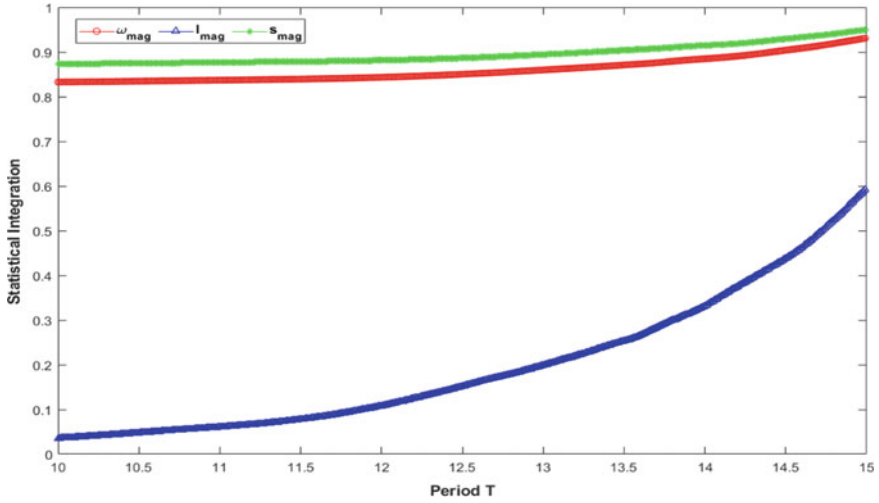
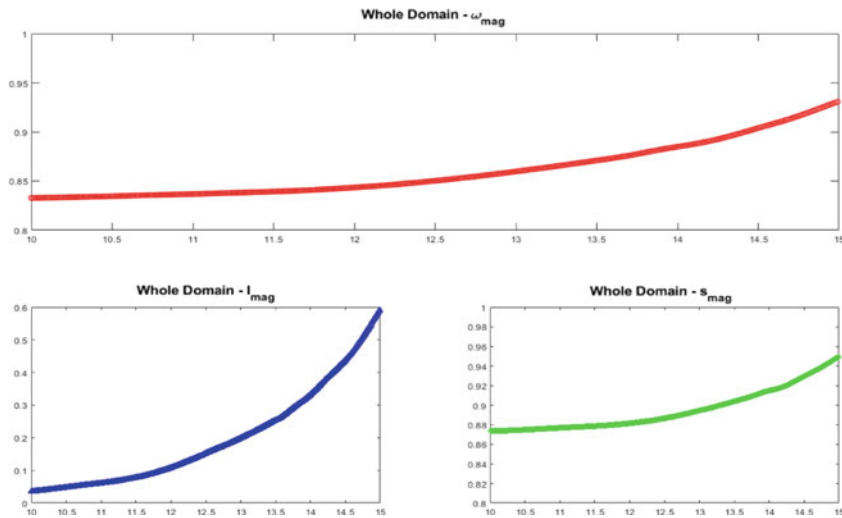**Fig. 11.5** Relative integration values for ω_{mag}, l_{mag} & s_{mag} plotted over time domain **T**

Fig. 11.6 Relative integration values for ω_{mag}, l_{mag} & s_{mag} plotted over time domain **T** - **individual graphs**

References

1. C. Liu, Y. Yun, P. Lu, Physics of turbulence generation and sustenance in a boundary layer. Comput. Fluids **102**, 353–384 (2014)
2. A. Perry, M. Chong, A Description of eddying motions and flow patterns using critical-point concepts. Annu. Rev. Fluid Mech. **19**(1), 125–155 (1987)

3. M.S. Chong, A.E. Perry, A general classification of three-dimensional flow fields. Phys. Fluids A: Fluid Dyn. **2**(5), 765–777 (1990). https://doi.org/10.1063/1.857730
4. J. Hunt, A. Wray, P. Moin, Eddies, stream, and convergence zones in turbulent flows (Center for Turbulent Research, 1988), pp. 193–208
5. J. Jeong, F. Hussain, On the identification of a vortex. J. Fluid Mech. **285**, 69–94 (1995). https://doi.org/10.1017/s0022112095000462
6. J. Zhou, R. Adrian, S. Balachandar, T. Kendall, Mechanisms for generating coherent packets of hairpin vortices in channel flow. J. Fluid Mech. **387**, 353–396 (1999)
7. C. Liu, Y. Wang, Y. Yang, Z. Duan, New omega vortex identification method. Sci. China Phys. Mech. Astron. **59**(8), 684711 (2016)
8. X. Dong, S. Tian, C. Liu, Correlation analysis on volume vorticity and vortex in late boundary layer transition. Phys. Fluids **30**(1), 014105 (2018). https://doi.org/10.1063/1.5009115
9. C. Liu, Y. Gao, S. Tian, X. Dong, Rortex-a new vortex vector definition and vorticity tensor and vector decompositions. Phys. Fluids **30**(3) (2018). https://doi.org/10.1063/1.5023001
10. Y. Gao, C. Liu, Rortex and comparison with eigenvalue-based vortex identification criteria. Phys. Fluids **30**(8), 085107 (2018)
11. P. Shrestha, C. Nottage, Y. Yu, Stretching and shearing contamination analysis for Liutex and other vortex identification methods. Adv. Aerodyn. **3**(8) (2021)
12. H. Helmholtz, On the integrals of the hydrodynamic equations corresponding to vortex motions. Journal für die reine und angewandte Mathematik (Crelles Journal) **55**, 22–25 (1858)
13. C. Liu, Y.-S. Gao, X.-R. Dong, Y.-Q. Wang, J.-M. Liu, Y.-N. Zhang, N. Gui, et al. Third generation of vortex identification methods: omega and Liutex/Rortex based systems. J. Hydrodyn. **31**, 205–223 (2019). https://doi.org/10.1007/s42241-019-0022-4
14. J. Wang, Y. Gao, C. Liu, Explicit formula for the Liutex vector and physical meaning of Vorticity based on the Liutex-Shear decomposition. J. Hydrodyn. **31**(3), 464–474 (2019)
15. Y. Yu, P. Shrestha, C. Nottage, C. Liu, Principal coordinates and principal velocity gradient tensor decomposition. J. Hydrodyn. **32**, 441–453 (2020)
16. C. Nottage, Y. Yu, P. Shrestha, C. Liu, Dimensional and theoretical analysis of second-generation vortex identification methods, in *Liutex and Third Generation of Vortex Definition and Identification.* ed. by C. Liu, Y. Wang (Springer, Cham, 2021), pp. 57–70
17. Y. Yan, C. Chen, F. Huankun, C. Liu, DNS study on Λ-vortex and vortex ring formation in the flow transition at Mach number 0.5. J. Turbul. **15**(1), 1–21 (2014)